RAA 2021 Vol. **21** No. **7**, 163(7pp) doi: 10.1088/1674-4527/21/7/163

http://www.raa-journal.org *http://iopscience.iop.org/raa*

***R**esearch in*
***A**stronomy and*
***A**strophysics*

Azimuth Control for Large Aperture Telescope Based on Segmented Arc Permanent Magnet Synchronous Motors

Xiao-Li Song[1,2], Da-Xing Wang[1,2] and Wang-Ping Zhou[3]

[1] Nanjing Institute of Astronomical Optics & Technology, National Astronomical Observatories, Nanjing 210042, China; *xlsong@niaot.ac.cn*
[2] CAS Key Laboratory of Astronomical Optics & Technology, Nanjing Institute of Astronomical Optics & Technology, Nanjing 210042, China
[3] School of Automation, Nanjing University of Information Science & Technology, Nanjing 210044, China

Received 2020 December 4; accepted 2021 February 4

Abstract A tracking control algorithm based on active disturbance rejection controller (ADRC) is proposed to overcome the telescope's mount fluctuation. The fluctuations are caused by internal and external disturbance when the large aperture telescope runs at ultra-low speed with direct drive. According to the high-precision and high-stability requirements of a large aperture telescope, the ADRC position controller is designed based on segmented arc Permanent Magnet Synchronous Motors (arc PMSMs). The tracking differentiator of ADRC is designed to undergo a transition process to avoid overshoot in the position loop. The speed of target tracking process is observed by the extended state observer and the position information in the system is estimated in real time. The current control variable of the segmented arc PMSM is generated by implementing a non-linear state error feedback control law. The simulation results demonstrate that the proposed control strategy can not only accurately estimate the position and speed of the tracking target, but also estimate the disturbance to compensate the control variables. Experiments showed that the speed error is less than $0.05'' \, s^{-1}$ when using the ADRC, and it can realize high tracking performance when compared with PID controller, which improves the robustness of a large aperture telescope control system.

Key words: techniques: telescopes — instrumentation: miscellaneous — methods: miscellaneous — techniques

1 INTRODUCTION

The control systems of large aperture ground-based telescopes differ somewhat from those of small/space-based telescopes because of the different nature of disturbances encountered. It is hard to ignore the external and internal disturbances for a large aperture optical telescope. Disturbances include external torques such as those due to wind or space environment and internal torques like backlash, friction in the bearings, cogging torque and changes in the moment of inertia of the telescope and instruments (Bely 2003).

A large aperture telescope servo control system should resist the disturbance torques that are mentioned above to overcome tracking jitter to ensure higher tracking performance. In recent years, many large aperture optical/infrared telescopes were constructed around the world, and segmented permanent magnet arc motors were adopted as the optimal drive solution, such as in the Very Large Telescope (VLT) (Leonardi et al. 1994) and the Gran Telescopio Canarias (GTC) (Cavaller & Siegel 2006). The European Extremely Large Telescope (E-ELT), when completed, will be the world's largest optical/infrared telescope. It also plans to incorporate segmented motors to drive the telescope axes by relying on the acquired experience of VLT and Atacama Large Millimeter/submillimeter Array (ALMA) (Giacomel et al. 2008). All telescopes that are mentioned above choose segmented disk-shaped arc motors as the mount drive; because they have large output torques and their thrust is distributed along the structure, they can reduce installation time and improve reliability and maintainability.

To collect more visible light to study faint celestial bodies, designs for next-generation extremely large optical

telescopes with primary mirror diameters ranging from 20 to 100 m have been developed. They are always found on high mountains, deserts, islands, Antarctica or other harsh environments. Also, when telescopes become progressively larger, they have voluminous bodies, and are vulnerable to servo stiffness and lower resonant frequencies. In addition, more additional structures are needed for accurate observation. Therefore, they are very sensitive to disturbances. For a long time, researches have focused on the Proportional-Integral-Derivative (PID) controller in many telescopes. VLT installed a Proportional-Integral (PI) controller with a feed-forward loop and some filters in angular velocity loop and position loop (Ravensbergen 1994). The position controller of the Subaru telescope utilizes a Proportional (P) controller to adjust the tracking position according to the size of the error (Kanzawa et al. 2006). GTC selected a feed-forward loop with PI and a second order Butterworth filter in the amplifier current loop to avoid unacceptable current noise amplification, a dual-feedback PI controller with velocity and acceleration feed-forward actions and proportional damping, which also includes some filters in the position loop (Suárez et al. 2008). PI and Linear-Quadratic-Gaussian (LQG) methodologies are incorporated in the NASA Deep Space Network antenna control systems of the main axes to compensate the antenna-pointing errors (Gawronski 2001). A fuzzy adaptive PID was studied to suppress the vibrations in the system of telescope axes' drive (Lukichev & Demidova 2016). In their studies, the PID controller with a feed-forward loop was widely used for angular velocity control because of its simplicity. However, it is difficult for the VLT to resist wind disturbances, and the GTC is ineffective in controlling disturbance caused by extremely flukey wind and other uncertain sources that suddenly appear.

So, it is difficult to achieve high precision by relying on a classical PID controller for a large aperture telescope because of its complex structure, unpredictable wind disturbance and non-linear frictional disturbance. It is necessary to find an efficient method that can improve the tracking performance for large aperture telescopes. In this study, a large aperture telescope tracking control system, called the active disturbance rejection controller (ADRC), is designed to make the system more robust and less dependent on the detailed mathematical model of the physical process. It can estimate and compensate for unknown dynamics and disturbance in real time, such as the change in moment of inertia of the motor and wind disturbance.

Table 1 Parameters of Segmented Arc PMSM

No	Motor Item	Value	Unit
1	Peak Torque	87	KN m
2	Rated Torque	43.5	KN m
3	Back EMF Constant	90	KV Krpm^{-1}
4	Torque Constant	1500	N m A^{-1}
5	Rotor Inertia	18 000	kg m^{-2}
6	Electrical Inductance	1.2	H
7	Electrical Resistance	20	Ω
8	Diameter	4.2	m

2 STRUCTURE OF SEGMENTED ARC PMSM

2.1 Structure of Drive System

To solve the problems of disturbance and stabilization in the control system for the main axes, pre-research work about a 4.2-meter segmented arc Permanent Magnet Synchronous Motor (arc PMSM) is carried out according to the azimuth characteristics of a large aperture telescope. Figure 1 is the distribution of segmented arc PMSM. It is a large torque motor, powered by the segmented motors, supported by hydraulic bearings. The whole platform is composed of 16 sub-motors, including 12 motors and 4 tachometer generators; any of the sub-motors can work separately. It has cylindrical-shaped rotors and radial flux, so it features the traits of curved motors. Figure 2 displays the general view of a 4.2-meter segmented arc PMSM. The parameters of the motor are listed in Table 1. Erm & Seppey compared the useful torque and its ripple between segmented disk-shaped arc motors and segmented cylindrical-shaped curved motors. The results of comparison indicated that the cylindrical-shaped segmented arc PMSM has a greater useful torque, with smaller cogging torque than a disk-shaped arc motor of the same size (Erm & Seppey 2006). The conceptual design architecture of a large aperture telescope is illustrated in Figure 3, and the details of the structure can be seen in the reference "Mechanisms for the elevation structure of a giant telescope" (Hu et al. 2018). The azimuth and elevation structure includes the primary mirror, secondary mirror, tertiary mirror and instruments.

2.2 Mathematical Model of Segmented arc PMSM

According to the theory of PMSM, a 3-phase static reference is converted to $d-q$ (Direct axis – Quadrature axis) synchronous rotation reference by the $abc-dq$ conversion matrix. If a field oriented control strategy is adopted, the reference for axes of the two-phase synchronous rotation is utilized to develop segmented arc PMSM equations. The mathematical model of PMSM is derived under the assumption that saturation from eddy-

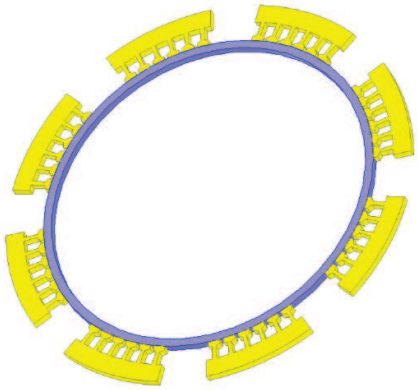

Fig. 1 Distribution schematic of segmented arc PMSM.

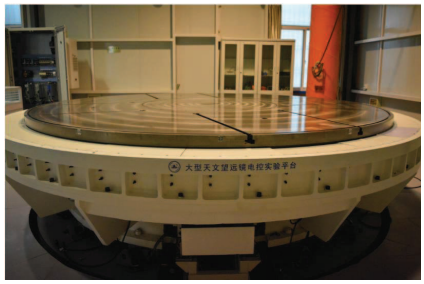

Fig. 2 General view of 4.2-meter segmented arc PMSM.

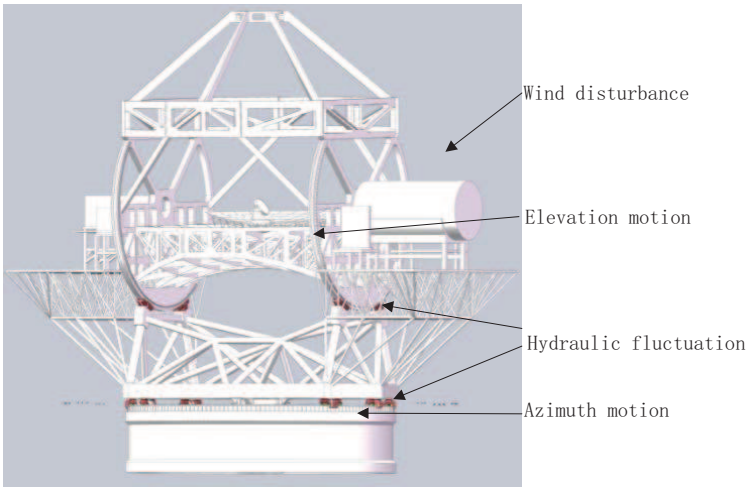

Fig. 3 Conceptual design architecture of large aperture telescope.

current high-order harmonic components is negligible, the stator windings are symmetric in space and that the stator currents produce sinusoidal magnetic motive forces. According to these assumptions, the differential equations of currents and electric angular velocity can be expressed as Equation (1) in $d-q$ synchronous rotating reference coordinate when the segmented arc PMSM is in a steady state.

$$\begin{cases} \frac{di_d}{dt} = \frac{1}{L_d}u_d - \frac{R_s}{L_d}i_d + \frac{L_q}{L_d}\omega_r i_q, \\ \frac{di_q}{dt} = \frac{1}{L_q}u_q - \frac{R_s}{L_q}i_q + \frac{L_d}{L_q}\omega_r i_d - \frac{1}{L_q}\omega_r\psi_f, \\ \frac{d\omega_r}{dt} = \frac{1}{J}p_n\psi_f i_q + \frac{1}{J}p_n(L_d - L_q)i_d i_q - \frac{1}{J}T_L - \frac{1}{J}B\omega_r, \end{cases} \tag{1}$$

where i_d, i_q, u_d and u_q are stator currents and voltages, respectively, in $d-q$ synchronous rotating reference coordinate, L_d and L_q are $d-q$ axes inductances, R_s is the stator armature resistance, ω_r is the electrical angular velocity of the rotor, Ψ_f is rotor flux, J is the moment of inertia, B is the viscous friction coefficient, T_L is the load torque and p_n is number of pole pairs.

From the differential equation describing the electric angular velocity, we can notice that velocity is influenced by the variables of stator current i_d and i_q, the load torque T_L and the viscous friction coefficient B. If the $i_d = 0$ strategy is adopted, the control structure of segmented arc PMSM is illustrated in Figure 4. Equation (1) can be simplified into

$$\begin{cases} \frac{di_q}{dt} = \frac{1}{L_q}u_q - \frac{R_s}{L_q}i_q - \frac{1}{L_q}\omega_r\psi_f, \\ \frac{d\omega_r}{dt} = \frac{1}{J}p_n\psi_f i_q - \frac{1}{J}T_L - \frac{1}{J}B\omega_r. \end{cases} \tag{2}$$

3 ADRC IN SEGMENTED ARC PMSM

The proposal for ADRC technology is derived from overcoming the disadvantage of PID control theory and creating a system to achieve high dynamic performance. Professor Han put forward the new concept of “Abandoning the old concepts of linearity and nonlinearity, giving full play to the power of feedback”. In recent years, it has established itself as a powerful control technology in dealing with the vast internal and external uncertainties arising from disturbance in

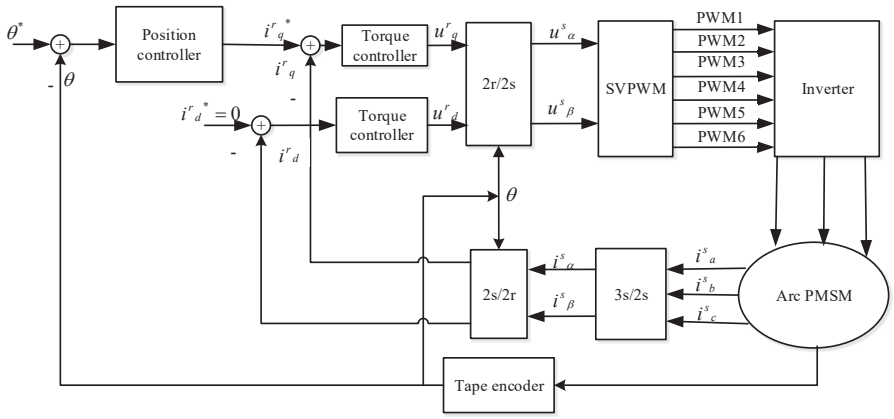

Fig. 4 Structure of segmented arc PMSM control system for a telescope.

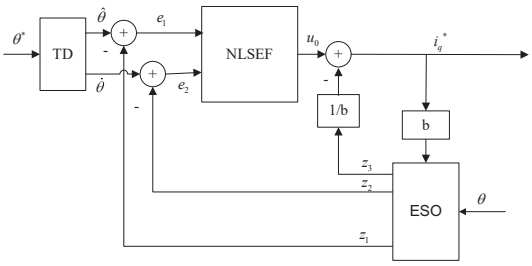

Fig. 5 Block diagram of ADRC position control.

control engineering. It can reject disturbance before it becomes a major problem. Researches show that it can adjust for changing variables and cancel the effects of disturbance. The theoretical system of ADRC consists of three parts which are the tracking differentiator (TD), the extended state observer (ESO) and the non-linear state error feedback (NLSEF) control law (Han 2009; Zhang & Han 2000; Ye et al. 2017).

3.1 Tracking Differentiator

For a non-linear second order system, with unknown disturbance, the state space equation of an uncertain object is as follows

$$\begin{cases} \dot{x}_1 = x_2 \\ \dot{x}_2 = f(x_1, x_2) + w(t) + bu \\ y = x_1 \end{cases}, \tag{3}$$

where $f(x_1, x_2)$ is an unknown system, w_t is an unknown disturbance, u is the input signal of the system, b is the gain of input signal and y is the output of the system.

In order to overcome the defects in classic differentiators, a transient process is necessary, which here is called TD. The TD introduces the idea of fastest control to track the input signal and then differentiates the tracking signal to obtain the approximate differential of the input signal. In addition to obtaining a high quality differential signal, it also has strong noise rejection ability and small phase lag, which solves the problem of noise amplification. The tracking of a step signal can sometimes enter the steady state without overshooting during a limited time. For a second order system, a discrete system is derived as

$$\begin{cases} r_1(k+1) = r_1(k) + h \cdot r_2(k) \\ r_2(k+1) = r_2(k) + h \cdot fhan(r_1(k) \\ \qquad\qquad - v(k), r_2(k), \delta, h_1) \end{cases}, \tag{4}$$

where $v(k)$ is the input signal at time k, $r_1(k)$ is the estimation of the input signal at time k, $r_2(k)$ is the estimation of the differential of the input signal at time k, δ and h_1 are controller parameters, h is the sampling step length ($h_1 > h$) and $fhan(\cdot)$ is the fastest control function, which can be described as

$$fhan(\cdot) = -\delta \begin{cases} a/d & |a| \le d \\ \mathrm{sgn}(a) & |a| > d \end{cases}, \tag{5}$$

where $\mathrm{sgn}(\cdot)$ is the sign function, and a and d are means of

$$\begin{cases} d = \delta h, d_0 = dh, y = r_1 + hr_2 \\ a = \begin{cases} r_2 + \mathrm{sgn}(y) * (a_0 - d)/2 & |y| > d_0 \\ r_2 + y/h & |y| \le d_0 \end{cases} \\ a_0 = \sqrt{d(d + 8\delta\,|y|)} \end{cases}. \tag{6}$$

Equation (4) is a time optimal solution that guarantees the fastest convergence from $r_1(k)$ to $v(k)$ and $r_2(k)$ to $\dot{v}(k)$. Also, the differentiator can filter noise when $v(k)$ is a signal with some noise.

3.2 Extended State Observer

ESO, which was proposed by professor Han, is such a method that can filter the output signal, reduce the influence of sensor noise, estimate the differential of the output signal and can estimate all the disturbances that affect the output of the system. For a large aperture

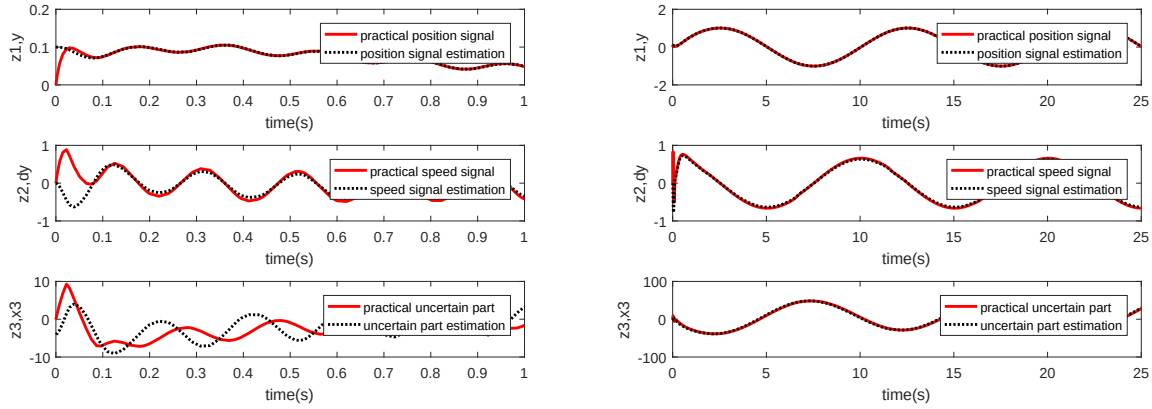

(a) When the frequency of input signal is 5 Hz

(b) When the frequency of input signal 0.1 Hz

Fig. 6 Plot of simulated position and speed tracking of ADRC.

Fig. 7 The hardware of drive and control.

telescope, the tracking accuracy greatly depends on the quantities of total disturbances estimated by the ESO.

For a system described by Equation (3), it can be supposed that $x_3 = f(x_1, x_2) + w(t), u = (u_0 - a(t))/b$. Here, $a(t)$ represents the combined effect of internal dynamics and external disturbance, i.e., the total disturbances. However, it is very difficult to know the exact value of $a(t)$ in practical engineering. Then, a new extended variable is equivalent to the total disturbance, which is always observable, and the plant can be built as

$$\begin{cases} \dot{x}_1 = x_2 \\ \dot{x}_2 = x_3 + bu \\ \dot{x}_3 = a(t) \\ y = x_1 \end{cases}. \tag{7}$$

Now, according to the effect of non-linear feedback, a state observer is constructed and ESO of the plant is expressed as

$$\begin{cases} e = z_1 - x_1 \\ z_1 = z_2 - \beta_1 fal(e, \alpha_1, \delta) \\ z_2 = z_3 - \beta_2 fal(e, \alpha_2, \delta) + bu \\ z_3 = \beta_3 fal(e, \alpha_3, \delta) \end{cases}, \tag{8}$$

where β_i is observer gains - there are many ways to select the values of the parameter, y is the output of the system, $z_1(t)$ and $z_2(t)$ are the observed state variables of ESO and $z_3(t)$ is the total disturbance of the system observed by ESO. The $fal(\cdot)$ is the saturation function whose purpose is to inhibit signal chattering, which takes the form

$$fal(e, \alpha, \delta) = \begin{cases} \frac{e}{\delta^{\alpha-1}}, & |e| \le \delta \\ |e|^{\alpha} \operatorname{sgn}(e), & |e| > \delta \end{cases}, \tag{9}$$

where e is the difference between output and input, α is the linear factor and δ is the filter coefficient. When $\alpha < 1$, the function of $fal(\cdot)$ has the characteristics of small error with large gain and large error with small gain to make the controller more efficient.

As long as the total disturbance is bounded, ESO can effectively estimate the state of the system, that is $z_1(t) \to x(t), z_2(t) \to \dot{x}(t)$ and $z_3(t) \to a(t)$.

3.3 Non-linear State Error Feedback Control Law

The NLSEF control law is developed from error feedback of the classical PID control method, which is independent of the nominal mathematical model. The NLSEF control law deals with the difference between the tracking signal generated by the TD and the differential signal of each order and the estimated value of the state variable generated by ESO, and combines it with the estimated value of the total disturbance of the system by ESO to form the control quantity of the system. Furthermore, it does not need to eliminate the steady error caused by the external disturbance and avoid the disadvantages such as phase lag, saturation and overshoot caused by integration. For a second order system, the control variable can be described as

$$\begin{cases} e_1 = x_1 - z_1 \\ e_2 = x_2 - z_2 \\ u_0 = \beta_{01} fal(e_1, \alpha_1, \delta) + \beta_{02} fal(e_2, \alpha_2, \delta) \\ u = u_0 - z_3/b \end{cases}. \tag{10}$$

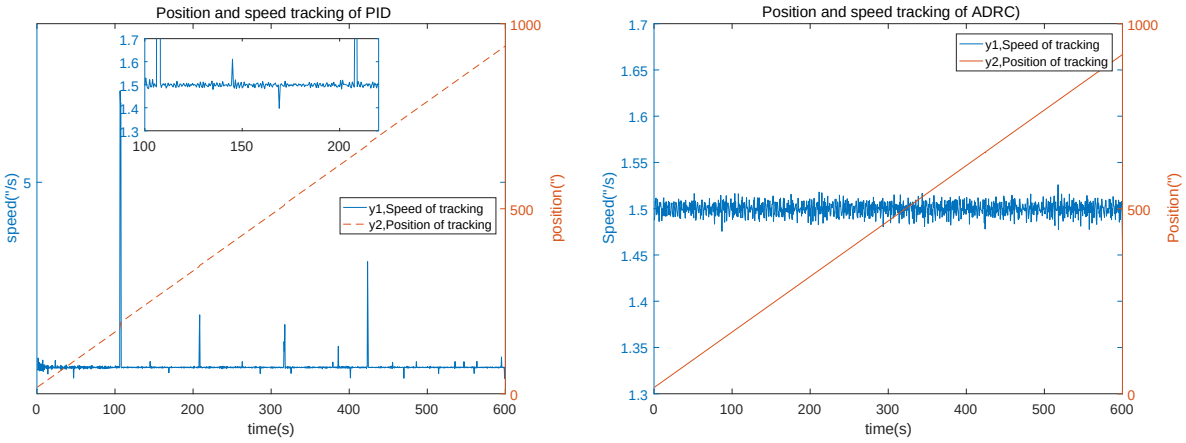

(a) PID controller (b) ADRC controller

Fig. 8 Actual position and speed tracking performance under PID and ADRC in the case of $1.5''\,\mathrm{s}^{-1}$ reference speed.

According to the theory of ADRC, the large aperture telescope position controller is designed as diagrammed in Figure 5. Here, θ is the target tracking position of the telescope, θ^* is the target's reference position, $\hat{\theta}$ is the estimated target's position through TD, $\dot{\theta}$ is the tracking angular velocity and z_3 is the disturbance of the tracking position. In light of the angular velocity being the derivative of position, if i_q is the control variable, the dynamic mathematical models of position loop can then be governed by an equation of second-order, the form of which is

$$\frac{d^2\theta}{dt^2} = \frac{d\omega}{dt} = \frac{1}{J}p_n\psi_f i_q - \frac{1}{J}T_L - \frac{1}{J}B\omega_r\ . \qquad (11)$$

Define the position of the segmented arc PMSM $\theta_1 = x_1$ and $\omega_r = x_2$, here, θ is detected by the tape encoder. Suppose that $f(x_1, x_2, t, w(t)) = -B\omega_r/J - T_L/J$ and $y = x_1$. Because $\hat{\theta} = \omega_r$, the non-linear state equations of segmented arc PMSM rotor position are

$$\begin{cases} \dot{x}_1 = \omega_r = x_2 \\ \dot{x}_2 = f(x_1, x_2, t, w(t)) + bu = a(t) + bi_q \\ y = x_1 \end{cases}, \qquad (12)$$

where $a(t) = -B\omega_r/J - T_L/J$ and $b = p_n\Psi_f$. According to the ADRC theory, Equations (8) and (10) can be used as ESO and NLSEF control laws.

4 SIMULATION AND EXPERIMENT

The segmented arc PMSM position servo control system is a double loop to estimate the position of the large aperture telescope and the result of its derivative (i.e., the angular velocity). A sinusoidal photoelectric scanning tape encoder with distance-coded absolute reference marks is installed for azimuth axis position feedback.

For a large aperture telescope, it is difficult to achieve accurate position and real-time estimation of the disturbance because of its large moment of inertia and its non-linear dynamic characteristics. Meanwhile, the tracking signal of position will lag the input signal when the frequency is high, and the unknown disturbance is also lagged. Therefore, the steady state precision of the system will be influenced. Figure 6 plots the simulation results of position and the estimation of tracking angular velocity when the input signal's frequency is different. It can be seen that the response bandwidth of the position loop is very narrow because of the large quality and moment of inertia.

To demonstrate the performance of the ADRC controller, several experiments have been done between the PID and ADRC controller based on the 4.2-meter segmented arc PMSM. Figure 7 depicts the hardware of drive and control system for the segmented arc PMSM. Figure 8 displays a comparison of two methods for the position and speed tracking performance when the objective speed is $1.5''\,\mathrm{s}^{-1}$. It can be observed that the speed error is bigger than $5''\,\mathrm{s}^{-1}$ when the controller is PID and the speed error is less than $0.05''\,\mathrm{s}^{-1}$ when the controller is ADRC. Also, the PID and $H\infty$ were experimented on in the same laboratory on the same plant, and the results can be seen in the "$H\infty$ controller design for a 4-meter direct-drive azimuth axis" (Chen et al. 2015).

5 CONCLUSIONS

In recent years, ADRC theory has stood out among various control systems due to its advantages in a complex uncertain physical system. In this paper, the proposed control strategy (i.e., ADRC) estimates the position of a tracking target without a nominal mathematical model

of the segmented arc PMSM and the total disturbance for the large aperture telescope. The results demonstrate that ADRC can ensure the robustness and adaptability under mathematical uncertainties if the total disturbance is unknown. It can observe the position of segmented arc PMSM and estimate the angular velocity and position of the tracking target.

Acknowledgements This work was supported by the National Natural Science Foundation of China (Grant Nos. 11673045 and 11573046). The authors gratefully acknowledge the support of National Astronomical Observatories/Nanjing Institute of Astronomical Optics & Technology, Chinese Academy of Sciences, and Prof. Zhenlian Zhu, Dr. Yu Ye and Dr. Shouwei Hu for the helpful discussion about segmented arc PMSM and structure of the large aperture telescope.

References

Bely, P. Y. 2003, The Design and Construction of Large Optical Telescopes (Springer New York)
Cavaller, L., & Siegel, B. 2006, in SPIE, 6267, 62673N
Chen, L., Zhang, Z., Song, X., & Wang, D. 2015, RAA (Research in Astronomy and Astrophysics), 15, 1931
Erm, T. M., & Seppey, A. 2006, in SPIE, 6273, 627335
Gawronski, W. 2001, IAPM, 43, 52
Giacomel, L., Manfrin, C., & Marchiori, G. 2008, in SPIE, 7012, 701236
Han, J. 2009, ITIE, 56, 900
Hu, S., Song, X., & Zhang, H. 2018, PASJ, 70, 52
Kanzawa, T.and Tomono, D., Usuda, T., Takato, N., et al. 2006, in SPIE, 6267, 62673J
Leonardi, F., Venturini, M., & Vismara, A. 1994, in IASAM, 2, 272
Lukichev, D. V., & Demidova, G. L. 2016, in ICPDS, 1
Ravensbergen, M. 1994, in SPIE, 2199, 997
Suárez, M., Rosich, J., Ortega, J., & Pazos, A. 2008, in SPIE, 7019, 70190J
Ye, Y., Yue, Z., & Gu, B. 2017, JINST, 12, T03006
Zhang, R., & Han, J. 2000, CTA, 17, 79